Treatment of the *K*-Quantum Number in Unimolecular Reaction Theory: Insights from Product Correlations

W. Sean McGivern and Simon W. North*

*Contribution from the Department of Chemistry, Texas A&M University,
3255 TAMU, College Station, Texas 77842*

Received June 18, 2002

Abstract: The connection between the *K*-quantum number and product correlations in the barrierless unimolecular dissociation of symmetric-top molecules is explored to establish a qualitative diagnostic for the treatment of the *K*-rotor dynamics in unimolecular reaction theory. We find that fragment scalar and vector correlations can provide guidance in this matter, and the photodissociation dynamics of thermal NCNO to form CN and NO at several dissociation wavelengths are presented to demonstrate the utility of this approach. The "goodness" of the *K*-quantum number can be related to the amount of energy in the conserved vibrational modes at the inner transition state. On the basis of measured correlated vibrational distributions, the *K*-quantum number is found to be approximately conserved at the inner transition state for the photodissociation of NCNO at 514, 520, and 526 nm. The methodology, involving a comparison of product distributions from the photodissociation of jet and thermal ensembles at identical wavelengths, is general and may be applied to previously studied systems that dissociate along barrierless potential energy surfaces, CF_3NO and CH_2CO. In addition, vector correlations serve as a means to probe the *K*-mixing at the outer transition state, and measured **v**−**j** correlations in the photodissociation of thermal NCNO are presented.

Introduction

Unimolecular reactions occurring along barrierless potential energy surfaces represent an important class of reactions that are of fundamental importance in atmospheric, interstellar, and combustion chemistry. The ability to accurately model these reactions is necessary for studying systems that are intractable to examine experimentally because of extreme conditions or complexity. A number of statistical theories have been developed to provide both rate constants and product distributions for this type of reaction.[1-3] These theories are derived from the tenet that only information regarding the reactant and the transition state is required to calculate rate constants and product quantum state distributions. Although the derivation of these theories is based on dynamical considerations, their implementation only requires the specification of a small number of constants of the motion.

The workhorse for predicting microcanonical rate constants, Rice−Ramsperger−Kassel−Marcus (RRKM) theory, typically specifies only the reaction energy, *E*, and the reactant rotational angular momentum quantum number, *J*:

$$k(E,J) = \frac{N^\ddagger(E-E_0,J)}{h\rho(E,J)} \qquad (1)$$

where $k(E,J)$ is the microcanonical rate constant, E_0 represents the threshold energy, $N^\ddagger(E-E_0,J)$ is the sum of states of the transition state, $\rho(E,J)$ is the density of states of the reactant molecule, and *h* is Planck's constant. As computational tech-

niques have become more powerful, greater detail of the reactant and transition-state structures and energetics required for eq 1 has become available, allowing accurate rate constants and product state distributions to be calculated. However, the accuracy of the calculated molecular properties has increased the need to correctly incorporate other quantities to refine the calculated rate constants further. The angular momentum of the *K*-rotor, described by the projection of the total angular momentum vector, **J**, on the symmetry axis of symmetric top, is such a quantity. Hase has recently noted that the proper treatment of the *K*-rotor in both the reactant and the transition state remains an important unsolved issue in unimolecular rate theory.[1,2,4-6]

The treatment of the *K*-quantum number is particularly important in the study of thermal association rate constants where the reaction rates are a strong function of the pressure.[5,6] In the high-pressure limit, the expression for the thermal rate constant is independent of the nature of the *K*-rotor if the reaction occurs over a barrier. However, on a barrierless potential, where the location of the transition state in an RRKM calculation is given by the point at which the sum of states of the transition state is a minimum, the high-pressure limiting rate

(1) Holbrook, K. A.; Pilling, M. A.; Robertson, S. H. *Unimolecular Reactions*, 2nd ed.; Wiley-Interscience, New York, 1996.
(2) Baer, T.; Hase, W. L. *Unimolecular Reaction Dynamics*; Oxford University Press: New York, 1996.
(3) Truhlar, D. G.; Garrett, B. C.; Klippenstein, S. J. *J. Phys. Chem.* **1996**, *100*, 12771.
(4) Hase, W. L. *Acc. Chem. Res.* **1998**, *31*, 659.
(5) Zhu, L.; Chen, W.; Hase, W. L.; Kaiser, E. W. *J. Phys. Chem.* **1993**, *97*, 311.
(6) Zhu, L.; Hase. W. L. *Chem. Phys. Lett.* **1990**, *175*, 117.

* Address correspondence to this author. E-mail: swnorth@tamu.edu.

constant is dependent on whether the *K*-rotor is active or adiabatic.[6] In the low-pressure limit, the rate is found to be strongly dependent on the treatment of the *K*-quantum number irrespective of the type of potential energy surface. In general, rate constants will be overestimated if a *K*-adiabatic system is treated with an active *K*-rotor. Additionally, the physical interpretation of the collisional efficiency derived from fitting low-pressure falloff data is strongly dependent on the treatment of the *K*-quantum number.[4] The study of *K*-mixing is therefore critical both to allow accurate modeling of unknown reaction rates and to understand the physics of thermal association reactions.

The "goodness" of the *K*-quantum number has been explored in numerous studies on the spectroscopy of highly excited molecules.[7] One finds that the mixing of the *K*-levels is substantial for excitation to states near the dissociation limits for a number of small molecules.[8,9] Above the threshold there is a competition between the time scales of *K*-mixing and unimolecular reaction. Few studies, however, have been able to address the nature of the *K*-rotor above dissociation thresholds.[10-13] Several of these have involved optical—optical double-resonance experiments in molecular beams which are limited to low *J* and *K* and are fundamentally different from thermal systems where higher-order Coriolis coupling terms can be important. Although most rate calculations have assumed that *K* is not a good quantum number (*K*-active model), it is difficult to distinguish between treatments of *K* based on kinetics data due to the uncertainty in several of the other inherent assumptions.[4]

It is well-known that scalar and vector correlations can provide significant insight into the dynamics of direct photodissociation reactions that occur on excited-state potential energy surfaces, which are often characterized by a localized release of potential energy into product translational motion.[14,15] More recently, the study of scalar and vector correlations has also been shown to be a powerful means to examine dissociation reactions along barrierless potentials.[16-22] We find that the study of product scalar and vector properties from thermal systems near vibrational thresholds provides a means to examine the nature of the *K*-rotor angular momentum. Marcus has qualitatively described a physical mechanism by which energy is partitioned among the vibrational and rotational energy levels in a barrierless reaction.[23] The conserved-mode vibrational

distribution is determined early in the reaction at the so-called "inner" transition state and maps directly to the products. In a thermal sample prior to optical excitation, the parent symmetric-top molecules have a broad distribution of parent rotational quantum states, *J*, but have restricted values of *K*. Coriolis coupling of the rotational motion to the vibrations of the molecule will result in a significant broadening of the *K*-distribution. The coupling of vibrational motion into rotation results in a significant change in the vibrational energy of the conserved modes at the inner transition state, which yields a different product vibrational distribution from that of a *K*-adiabatic system. The transitional modes remain coupled until the system reaches the "outer", orbiting, transition state.[24] Constraints may be manifested in the rotational distributions, but vector correlations, specifically those between the relative velocity, **v**, and the product rotational angular momentum vector, **j**, have been shown to be a sensitive probe of the *K*-rotor activity at the outer transition state.[13,19] The activity of the *K*-rotor strongly affects the sum of states at this transition state, which is important for calculating rates for reactions just above vibrational thresholds.[25,26,29,30]

We have recently examined the fragment correlations in the photodissociation of room temperature nitrosyl cyanide (NCNO) using transient frequency modulation Doppler spectroscopy at 520 nm.[27] The present study represents an extension of that work to include other wavelengths that span a range of dissociation lifetimes. On the basis of these additional results, we believe that this method for probing the *K*-rotor dynamics at the inner transition state may be applied to other systems that undergo barrierless unimolecular dissociation. To this end, we have examined previous work by other groups on two prototypical systems for barrierless unimolecular reactions, CF_3NO and CH_2-CO. We find that both systems show evidence for approximate *K*-mixing, which is qualitatively consistent with the rates of dissociation relative to the rotational periods of the parent molecules as well as their relative densities of reactant states.

Experiment

The transient frequency modulation (FM) Doppler spectroscopy technique used in the NCNO studies has been described in detail previously.[27,28,56,57] Briefly, the output of a near-infrared diode laser operating on the A—X electronic transitions of CN near 800 nm was frequency modulated using an electrooptic phase modulator. The frequency-modulated beam primarily consists of the fundamental and two sideband frequencies, equally spaced above and below the fundamental, that are 180° out of phase. Preferential absorption of one of the sidebands causes amplitude modulation at the sideband spacing frequency, 192 MHz in the present experiment. This spacing is significantly less than the width of the absorption features of interest, and scanning the output of the laser over a single rotational state provides a spectrum that is a near derivative of the absorption feature. The photolysis beam was generated from a Nd:YAG-pumped dye laser operating with Coumarin 500 dye. The sample is introduced via a needle valve into a long-path-length absorption cell at pressures of 10—30 mTorr, and the photolysis and probe beams propagate collinearly along

(7) Hamilton, C. E.; Kinsey, J. L.; Field, R. W. *Annu. Rev. Phys. Chem.* **1986**, *37*, 493.
(8) Abramson, E.; Field, R. W.; Imre, D.; Innes, K. K.; Kinsey, J. L. *J. Chem. Phys.* **1985**, *83*, 453.
(9) Dai, H. L.; Korpa, C. L.; Kinsey, J. L.; Field, R. W. *J. Chem. Phys.* **1985**, *82*, 1688.
(10) Mellinger, A.; Ashikmin, M. V.; Moore, C. B. *J. Chem. Phys.* **1998**, *108*, 8944.
(11) Ionov, P. I.; Bezel, I.; Ionov, S. I.; Wittig, C. *Chem. Phys. Lett.* **1997**, *272*, 257.
(12) Bezel, I.; Ionov, P.; Wittig, C. *J. Chem. Phys.* **1999**, *111*, 9267.
(13) North, S. W.; Hall, G. E. *Ber. Bunsen-Ges. Phys. Chem.* **1997**, *101*, 496.
(14) Sato, H. *Chem. Rev.* **2001**, *107*, 2687.
(15) Hall, G. E.; Houston, P. L. *Annu. Rev. Phys. Chem.* **1989**, *40*, 375.
(16) Nadler, I.; Pfab, J.; Reisler, H.; Wittig, C. *J. Chem. Phys.* **1984**, *81*, 653.
(17) Qian, C. X. W.; Noble, M.; Nadler, I.; Reisler, H.; Wittig, C. *J. Chem. Phys.* **1985**, *83*, 5573.
(18) Qian, C. X. W.; Ogai, A.; Reisler, H.; Wittig, C. *J. Chem. Phys.* **1989**, *90*, 209.
(19) North, S. W.; Hall, G. E. *J. Chem. Phys.* **1997**, *106*, 60.
(20) Costen, M. L.; Katayanagi, H.; Hall, G. E. *J. Phys. Chem. A* **2000**, *104*, 10247.
(21) Morgan, C. G.; Drabbels, M.; Wodtke, A. M. *J. Chem. Phys.* **1996**, *104*, 7460.
(22) Spasov, J. S.; Cline, J. I. *J. Chem. Phys.* **1999**, *110*, 9568.

(23) Marcus, R. A. *Chem. Phys. Lett.* **1988**, *144*, 208.
(24) An early reference to inner and outer transition states in barrierless dissociation can be found in Rai, S. N.; Truhlar, D. G. *J. Chem. Phys.* **1983**, *79*, 6046.
(25) Miller, W. H. *J. Chem. Phys.* **1976**, *65*, 2216.
(26) Klippenstein, S. J. *J. Chem. Phys.* **1994**, *101*, 1996
(27) McGivern, W. S.; North, S. W. *J. Chem. Phys.* **2002**, *116*, 7027.
(28) North, S. W.; Hall, G. E. *Annu. Rev. Phys. Chem.* **2000**, *51*, 243.
(29) Chesnavich, W. J.; Bowers, M. T. *J. Am. Chem. Soc.* **1977**, *99*, 1705.
(30) Chesnavich, W. J.; Bowers, M. T. *J. Chem. Phys.* **1977**, *66*, 2306.

its length. To ensure that Doppler spectra are acquired prior to translational or rotational relaxation of the CN radicals, the signal is sampled from the first 100 ns after the photolysis pulse. A fast photodiode is used to measure the high-frequency intensity variation, and standard phase-sensitive detection electronics are used to convert the magnitude of the beat signal to a dc voltage for analysis and archival.

Analysis and Discussion

In NCNO, the incident photon excites the system to the first singlet excited state, S_1. A large barrier to dissociation (>5000 cm^{-1}) exists on the S_1 surface, and for wavelengths >450 nm the system internally converts back to the ground state, where dissociation occurs.[31] A qualitatively similar dissociation mechanism is also present in CF_3NO and CH_2CO as discussed below.

Scalar Correlations and the *K*-Quantum Number. There are several prescriptions for calculating product state distributions in barrierless reactions.[1,2] The simplest theory, phase space theory (PST), assumes that both the conserved and transitional modes are strongly coupled throughout the dissociation, which is equivalent to locating a variational RRKM transition state at infinity.[32,33] The resulting product state distributions are thus simply determined by the degeneracies of the individual product quantum states. While PST has been successful at modeling rotational product state distributions at low energies in numerous systems, it typically overestimates rate constants and has been found to underestimate product vibrational excitation. A model that overcomes these shortcomings of PST assumes that the vibrational modes are strongly coupled only up to the inner transition state, at which point the conserved modes become adiabatic. The transitional modes, which evolve into fragment rotations, remain strongly coupled until a second outer transition state.[34] This separation of coupling regimes is the principle behind both the vibrationally adiabatic variational RRKM treatment of Marcus[23] and the separate statistical ensembles (SSE) method proposed by Wittig and co-workers.[35]

An accurate variational RRKM treatment of dissociation to vibrationally excited products requires a transition state to be located for each conserved-mode vibrational channel. Evaluation of the transition-state location at each ascending vibrational channel is performed at decreasing available energies to account for the energy in the individual product vibrations. The transition states become looser for each successively higher vibrational channel. This treatment provides a greater flux at each of the increasing vibrational levels relative to that of the ground state than would be expected from a PST calculation, where the transition states are all located at infinity. This greater relative flux for the vibrationally excited channels will therefore provide more vibrationally excited products than would be predicted using PST. The SSE model is an alternative to the RRKM treatment for calculating product state distributions without consideration of the rate constants. The SSE model utilizes the density of states of the "unhindered" vibrational degrees of freedom of the parent molecule to calculate the product vibrational distribution. The SSE model is equivalent to a pure PST model in which a third degree of freedom, in addition to
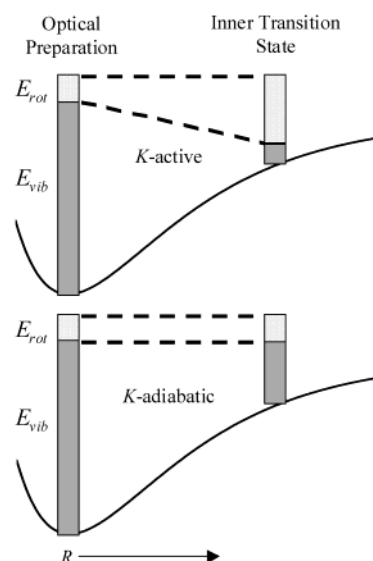

Figure 1. Schematic vibrational and rotational energies of the reactant and transition state in a prolate symmetric top. The dark gray areas represent the vibrational energy at each point along the reaction coordinate, and the light gray areas represent the rotational energy. In a *K*-adiabatic system, the change in the rotational energy between the reactant and transition state is small. *K*-mixing removes energy from the vibrational reservoir in a prolate top, causing less vibrational energy to be present at the inner transition state.

those removed to account for the reaction coordinate and angular momentum conservation, is removed.[2] A theoretical connection between the variational RRKM treatment and the SSE method is currently undeveloped.[36] We have chosen to use SSE in the present calculations because of its relative simplicity of implementation and previously demonstrated ability to describe the global product vibrational distributions derived from NCNO photodissociation.[17,18,31]

The principle of using scalar distributions to interrogate the nature of the *K*-rotor at the inner transition state relies on this model of the different coupling regimes associated with the conserved and transitional modes. Strong coupling of the *K*-rotor energy to the vibrational energy reservoir prior to the inner transition state would result in a uniform *K*-distribution when the vibrations become adiabatic, although the extent to which the *K*-rotor fully samples phase space remains an open question.[37] The effect of *K*-mixing on the product vibrational distributions is dependent on the geometry of the reactant molecule.[38] For a thermal sample of a prolate symmetric top, the *K*-distribution is peaked at zero, and randomization would be expected to remove energy from the vibrational energy reservoir, yielding cold vibrational distributions. A schematic diagram of the vibrational and rotational energies for the reactant and transition states of a prolate top is shown in Figure 1. For an oblate symmetric top, the *K*-distribution is peaked at the parent rotational quantum number, $\pm J$, and a uniform *K*-distribution would add energy to the vibrational energy reservoir prior to the inner transition state. In the present system, NCNO is a near-prolate symmetric top, so a *K*-active system would produce colder fragment vibrational distributions than if the system were *K*-adiabatic.

(31) Noble, M.; Nadler, I.; Reisler, H.; Wittig, C. *J. Chem. Phys.* **1984**, *81*, 4333.
(32) Pechukas, P.; Light, J. C. *J. Chem. Phys.* **1965**, *42*, 3281.
(33) Klots, C. E. *J. Phys. Chem.* **1971**, *75*, 1526.
(34) The applicability of the adiabatic treatment of the conserved-mode vibrations is uncertain for larger systems that have low-frequency vibrational modes.
(35) Wittig, C.; Nadler, I.; Reisler, H.; Noble, M.; Catanzarite, J.; Radhakrishnan, G. *J. Chem. Phys.* **1985**, *83*, 5581.

(36) Green, W. H., Jr.; Moore, C. B.; Polik, W. F. *Annu. Rev. Phys. Chem.* **1992**, *43*, 591.
(37) Perry, D. S.; Bethardy, G. A.; Davis, M. J.; Go. J. *Faraday Discuss.* **1995**, *102*, 215.
(38) Aubanel, E. E.; Wardlaw, D. M.; Zhu, L.; Hase, W. L. *Int. Rev. Phys. Chem.* **1991**, *10*, 249.
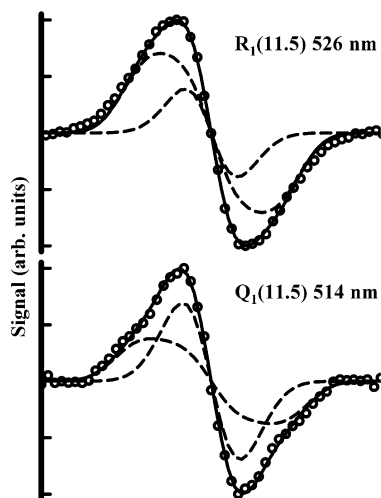
Figure 2. Typical FM Doppler spectra. The upper panel shows an R-branch for $j = 11.5$ CN radicals derived from the photodissociation of NCNO at 526 nm, and the lower panel shows a Q-branch for $j = 11.5$ CN from photodissociation at 514 nm. The data in the lower panel have been symmetrized to remove the effects of the R_{12} satellite transition. The circles represent experimental data. The dashed lines represented simulated Doppler profiles derived from PST rotational distributions for the coincident $v = 0$ and $v = 1$ NO fragments, and the solid lines are the best-fit weighted sums of these basis functions.

Correlated vibrational branching ratios are determined experimentally by first simulating Doppler profiles for each energetically available vibrational channel using PST. The details of this procedure are provided elsewhere.[27] The correlated vibrational branching ratios are then determined by weighting these basis functions to provide the best fit to the measured Doppler profiles. Figure 2 shows typical FM Doppler spectra at 514 and 526 nm and their corresponding fits. The circles represent experimental data. The dashed lines represent the simulated basis functions for the $v = 0$ and $v = 1$ channels, and the solid lines represent the best-fit weighted sum of the simulations.[27] The differences between these two contributions are significant, providing a robust method for determination of the correlated vibrational branching ratios. Shown in Figure 3 are correlated vibrational branching ratios determined from Doppler spectra for several CN rotational quantum states for the photodissociation of NCNO at three wavelengths. The 520 nm results have been reported previously.[27] The solid and dashed lines are the results of SSE theory under K-adiabatic and K-active conditions at the inner transition state, respectively. All of the simulations include thermal averaging to account for the internal energy distribution of the parent molecules at room temperature. We find that the K-adiabatic SSE values are significantly larger than the K-active values and provide the best fit to the experimental data at all wavelengths.[39] We therefore conclude that the K-rotor is not strongly coupled into the vibrational reservoir early in the reaction.

Although global vibrational branching ratios can provide similar information in principle, the use of correlated branching fractions has significant advantages. At excitation energies near the threshold for vibrational excitation, the differences between K-adiabatic and K-active global branching ratios are typically small and may be difficult to distinguish. Correlated studies examine larger differences between relative measurements rather
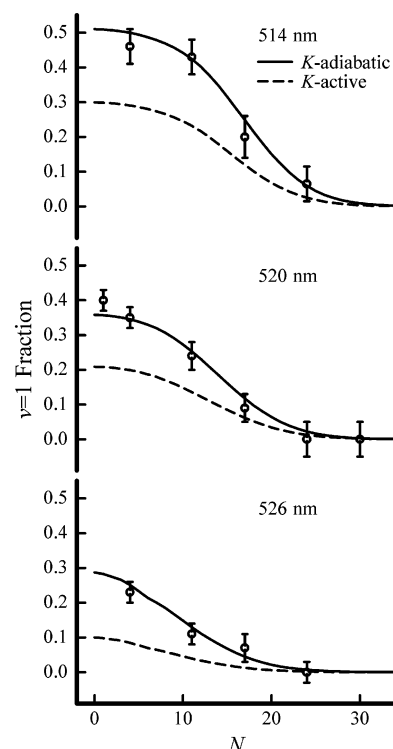
---

(39) The predictions of the K-active SSE model and PST are very similar for all wavelengths studied.

Figure 3. Correlated vibrational branching ratios at 526, 520, and 514 nm as a function of CN rotational quantum number N. Open circles represent experimental values. Solid and dashed lines are the simulations from SSE theory, where the K-quantum number is treated as adiabatic and active, respectively.

than the smaller differences in absolute measurements typically observed in the global branching ratios. At a correlated level, numerous independent measurements of the vibrational branching ratio may be made, corresponding to individual rovibrational states of the detected fragment, and can provide additional certainty in the measured values.

Numerous studies have identified SSE as an effective description of the energy partitioning of a dissociating system in a molecular beam. In the typical application of the SSE model, K-adiabaticity is implicit because only the parent thermal vibrational energy and the photon energy are used to determine the vibrational branching.[35] However, the use of an adiabatic K-rotor in an SSE calculation has little effect on the calculated vibrational branching of a sample in a molecular beam, since the rotational cooling of the parent precludes a detailed analysis of the K-rotor dynamics. The observation of significant changes in the vibrational branching ratio requires large values of J, the parent rotational quantum number, to ensure that the differences between the K-adiabatic and K-active cases are sufficient to permit unambiguous identification.

The photodissociation of ketene to give singlet CH_2 and CO is one of the most significant benchmarks for the study of unimolecular dissociation on barrierless potentials.[14] As with NCNO, vibrational branching ratios may distinguish between an active and adiabatic K-rotor. Global measurements of the CO vibrational distribution derived from the 308 nm photodissociation of room temperature ketene were made by Nesbitt et al. using laser-induced fluorescence.[40] Those authors measured a value of 0.09 ± 0.05 for the $(v = 1)/(v = 0)$ ratio of populations, which were found to be consistent with the SSE

model, which treated K as adiabatic implicitly. However, more recent correlated measurements have revealed that the global vibrational branching ratio may be significantly lower than the previously reported value.[41] The correlated CO vibrational branching ratio of jet-cooled CH_2CO has been measured recently by Costen et al.[20] Interestingly, the measured correlated vibrational branching ratios in the room temperature sample are the same or lower than the corresponding jet-cooled branching ratios for each measured CH_2 transition common to both studies, despite the additional vibrational energy that would be expected from the internal energy of the parent molecule in the room temperature sample. It is unlikely that changes in the global CH_2 rotational distribution could compensate for the factor of 3 increase in the correlated vibrational branching ratio predicted by the K-adiabatic SSE model in going from jet-cooled to room temperature parent molecules. We therefore believe that this difference may be indicative of approximate K-mixing at the inner transition state. Experiments are currently underway to remeasure the global CO vibrational distributions.

The differences between global branching ratios in the bulb and the molecular beam may still provide some insight into the nature of the K-rotor in systems for which correlated measurements of the vibrational branching have not been made. The photodissociation of CF_3NO to give CF_3 and NO provides an example in which the K-rotor appears to play an important role in the overall dynamics of the room temperature system. Although correlated measurements have been made by detecting the NO fragment to identify the wavelength-dependent photodissociation dynamics,[22] no studies of the correlated NO vibrational branching ratios have been undertaken. Like NCNO, CF_3NO is a near-prolate symmetric top, and dissociation occurs along the S_0 potential energy surface after internal conversion from the first singlet excited state when following excitation at wavelengths longer than 610 nm.[42-45] Houston and co-workers[44,45] measured global vibrational and rotational distributions for the photodissociation of both room temperature and jet-cooled CF_3NO at wavelengths ranging from 600 to 660 nm, corresponding to $1172-2687$ cm^{-1} of energy above the dissociation threshold.[46] At 625 nm, which corresponds to 111 cm^{-1} above the threshold for $v = 1$ formation in the NO fragment, a $(v = 1)/(v = 0)$ ratio for NO of 0.022 ± 0.011 was observed in a jet-cooled sample.[45] At room temperature, dissociation at the same wavelength resulted in a $(v = 1)/(v = 0)$ ratio for NO of 0.018 ± 0.009.[42] Although the differences are small and the estimated errors are relatively large, the room temperature sample would be expected to have a significantly larger vibrational branching ratio if the K-rotor were adiabatic as a result of the significant parent thermal vibrational energy. We suggest that this lower vibrational branching ratio in the bulb is a signature of K-mixing at the inner transition state, although clearly more experiments are necessary to confirm this hypothesis. It should be noted that the appearance rates for products from the photodissociation of CF_3NO are dominated

by internal conversion to the ground state. The extent to which K-mixing occurs on the ground or excited state is not revealed by measurements of the product distributions, which show only that K-mixing has occurred prior to reaching the inner transition state.

The mixing of the K-quantum number in a symmetric top requires the coupling of vibrational motion to rotational motion about the symmetry axis through either Coriolis coupling or Fermi interactions.[47] It is difficult to develop a general prescription for how to treat K in unimolecular dissociation since the competition between K-mixing and dissociation time scales will depend on numerous factors including the density of states, the magnitudes of J and K, and the dissociation rates. Perry et al. have examined the time scale of K-mixing in near-prolate symmetric tops and found that the scrambling of K to states near J requires several hundred rotations of the parent molecule.[37] Treating the frequency of parent rotation, ω, as a "conceptual limit" to the rate of Coriolis mixing as described by Perry et al.,[37] one would not expect significant K-mixing if ω were less than or equal to the dissociation rate. The dissociation rate of NCNO has been examined in detail both experimentally[48] and theoretically,[49-51] though these studies did not extend to the available energies of the present work. Variational RRKM calculations that are consistent with the previous studies at lower energies yield a unimolecular dissociation rate constant of 5×10^{11} s^{-1} for 520 nm photolysis. The average rate of rotation of NCNO, assuming it to be a symmetric top with a rotational constant for rotation about the axis perpendicular to the symmetry axis of 0.175 cm^{-1}, is 1.4 $\times 10^{12}$ s^{-1} at 295 K. This difference is sufficient to remove any significant laboratory frame anisotropy of the departing fragments; however, it is unlikely to be sufficiently long to allow extensive K-mixing to values near J in a thermal sample. As a result, the observation that K is approximately adiabatic at the inner transition state in NCNO dissociation is not unreasonable.

However, the unimolecular dissociation rates of CF_3NO and ketene are significantly slower and the state densities significantly larger than those of NCNO at wavelengths corresponding to a few hundred cm^{-1} above the threshold for formation of vibrationally excited diatomic fragments. The dissociation rates of CF_3NO at the wavelengths of interest in the studies by Houston and co-workers[44,45] were on the order of 10^7-10^8 s^{-1}. The average rotational frequency of CF_3NO at 295 K is 1.1 $\times 10^{12}$ s^{-1}, several orders of magnitude higher than the dissociation rate. K-mixing would be expected to be more extensive in CF_3-NO than in the faster NCNO dissociation, which is consistent with the postulated K-mixing mechanism apparent from the difference between the bulb and jet experiments. Similarly, the rate constant for the dissociation of ketene on the singlet potential energy surface was calculated to be 9×10^9 s^{-1} by Klippenstein et al. for 308 nm photodissociation.[52] At 295 K, the average rotational frequency of ketene is 2×10^{12} s^{-1}, still significantly higher than the dissociation rate. As in CF_3NO, K-mixing would be expected to take place prior to the inner

(40) Nesbitt, D. J.; Petek, H.; Foltz, M. F.; Filseth, S. V.; Bamford, D. J.; Moore, C. B. *J. Chem. Phys.* **1985**, *83*, 223.
(41) The analysis of the correlated distributions is unpublished, but a comparison of the jet and thermal Doppler spectra can be found in ref 28.
(42) Spears, K. G.; Hoffland, L. *J. Chem. Phys.* **1977**, *66*, 1755.
(43) Spears, K. G.; Hoffland, L. D. *J. Chem. Phys.* **1981**, *74*, 4765.
(44) Roellig, M. P.; Houston, P. L.; Asscher, M.; and Haas, Y. *J. Chem. Phys.* **1980**, *73*, 5081.
(45) Bower, R. D.; Jones, R. W.; Houston, P. L. *J. Chem. Phys.* **1983**, *79*, 2799.
(46) Spasov, J. S.; Cline, J. I. *J. Chem. Phys.* **1999**, *110*, 9568.

(47) Maessen, B.; Wolfsberg, M., *J. Chem. Phys.* **1984**, *80*, 4651.
(48) Khundkar, L. R.; Knee, J. L.; Zewail, A. H. *J. Chem. Phys.* **1987**, *87*, 77.
(49) Klippenstein, S. J.; Khundkar, L. R.; Zewail, A. H.; Marcus, R. A. *J. Chem. Phys.* **1988**, *89*, 4761.
(50) Klippenstein, S. J. *J. Chem. Phys.* **1991**, *94*, 6469.
(51) Klippenstein, S. J. *J. Chem. Phys.* **1992**, *96*, 367.
(52) Klippenstein, S. J.; East, A. L. L.; Allen, W. D. *J. Chem. Phys.* **1996**, *105*, 118.

transition state, although whether the mixing takes place in the ground- or excited-state surfaces is unknown. Some evidence for incomplete K-mixing in the near-threshold photodissociation of NO_2 has been observed previously using optical double resonance to measure rates from specific parent (J, K) states. The lack of complete K-mixing was attributed to the fast dissociation of NO_2 relative to the parent rotational period. Later classical trajectory calculations on this system confirmed this hypothesis, finding that several molecular rotations are necessary to obtain appreciable K-mixing.[53]

Vector Correlations and the K-Rotor. Vibrational distributions can provide no information on the dissociation dynamics after the conserved modes are decoupled at the inner transition state. However, vector correlations, namely, correlations among $\boldsymbol{\mu}$, the molecular transition dipole moment vector, $\mathbf{v}$, the relative velocity vector, and $\mathbf{j}$, the rotational angular momentum vector of the detected fragment, can provide detailed information on the long-range anisotropy of the potential and exit channel couplings. These long-range effects do not influence the rate constant except at energies close to vibrational thresholds but play a significant role in the product state distributions. Correlations involving $\boldsymbol{\mu}$ may be probed by utilizing a polarized laser for photolysis, which defines a preferred direction in the laboratory frame. An anisotropic distribution of photofragments in the laboratory frame of reference may be probed using several techniques, including laser-induced fluorescence, numerous mass spectrometric methods, and the transient FM method described in the present work. However, in the case of NCNO, the dissociation is sufficiently slow relative to the rotational period of the parent molecule that the correlation between the transition dipole moment of the parent molecule and the speed and rotation of the product molecules has disappeared. The correlation between $\mathbf{v}$ and $\mathbf{j}$ does not depend on the alignment in the laboratory frame and remains important.

The relationship between the $\mathbf{v}$–$\mathbf{j}$ correlations and K-mixing in barrierless unimolecular dissociation reactions has been discussed in detail by North and Hall.[13] Briefly, the K-quantum number may be related to the $\mathbf{v}$–$\mathbf{j}$ correlation by transforming the system into a basis in which the projections of the angular momenta of the fragments along the relative velocity vector are good quantum numbers. Since the relative velocity vector is strictly perpendicular to the orbital angular momentum of the fragments about the parent center of mass, these fragment projections map directly to the K-quantum number. In a K-active system, there is no restriction on the projection of the fragment angular momentum on $\mathbf{v}$, leading to small correlations between $\mathbf{v}$ and $\mathbf{j}$. K-adiabatic systems, however, are limited to only a small number of such projections and lead to strong correlations between $\mathbf{v}$ and $\mathbf{j}$. Experimentally, these correlations may be probed by examining the differences between Q- and R-branch transitions with the same initial rotational state.[54,55] We have previously reported the $\mathbf{v}$–$\mathbf{j}$ correlations in the 520 nm photodissociation of NCNO.[27] The $\mathbf{v}$–$\mathbf{j}$ correlations were found to be small and were well-represented by treating the system at the outer transition state as K-active. The $\mathbf{v}$–$\mathbf{j}$ correlations measured at 514 and 526 nm were also found to be small for

all measured rotational states, consistent with K-scrambling at the outer transition state.

The presence of a K-active outer transition state and a K-adiabatic inner transition state is surprising, since the system would be expected to pass between the inner and outer transition states in less than a picosecond. This motion would require strong Coriolis coupling to allow the K-quantum number to partially scramble on this time scale. While this is not altogether unreasonable, other factors may affect the magnitudes of the $\mathbf{v}$–$\mathbf{j}$ correlations. The strict relationship between the K-quantum number and the total projection of the rotational angular momentum vectors on the relative velocity axis is true only within the axial recoil approximation for a true symmetric top molecule. Significant rotation of the molecular complex as dissociation occurs allows states with different total projections along the relative velocity axis to mix, which would be expected to degrade the observed $\mathbf{v}$–$\mathbf{j}$ correlations. The dissociation axis and the symmetry axis of the near-symmetric top do not strictly coincide, which leads directly to an additional blurring of the $\mathbf{v}$–$\mathbf{j}$ correlation. Finally, the broadening of the observed Doppler spectra due to parent translational motion increases the overall uncertainty in the measured correlations. The measurement of $\mathbf{v}$–$\mathbf{j}$ correlations in a collimated effusive beam of room temperature molecules would significantly decrease the translational blurring, allowing a more accurate determination of the $\mathbf{v}$–$\mathbf{j}$ correlations, while maintaining the thermal parent rotational energy required to probe the nature of the K-rotor. These experiments are currently underway in our laboratory.

Conclusion

The extent of coupling of the K-rotor motion in barrierless unimolecular dissociation reactions has been examined by studying fragment correlations in the photodissociation of NCNO. We find that both product scalar and vector correlations can provide a diagnostic on the nature of the K-rotor in unimolecular dissociation, particularly when a comparison between results from jet and thermal experiments is possible. At three dissociation wavelengths, vibrational branching ratios of the NO radical were determined for several coincident CN rotational quantum states. The correlated vibrational branching ratios are found to be well-described by a separate statistical ensembles treatment in which the K-rotor is assumed to be adiabatic at the transition state. The use of vibrational distributions as a probe of K-rotor activity has been applied more generally to CF_3NO and CH_2CO, which were both found to be approximately K-active at the transition state. As expected, K-mixing appears to become more extensive as the dissociation rate decreases relative to the parent rotational period. Vector correlations, which serve as a probe of the K-rotor activity at the outer transition state, were also measured for NCNO photodissociation. The $\mathbf{v}$–$\mathbf{j}$ correlations were found to be small at both 514 and 526 nm, which is indicative of K-mixing at the outer transition state.

(53) Grebenshchikov, S. Y.; Flöthmann, H.; Schinke, R.; Bezel, I.; Wittig, C.; Kato, S. *Chem. Phys. Lett.* **1998**, *285*, 410.
(54) Hall, G. E.; Houston, P. L. *Annu. Rev. Phys. Chem.* **1989**, *40*, 375.
(55) Gordon, R. J.; Hall, G. E. *Adv. Chem. Phys.* **1996**, *96*, 1.
(56) Li, R.; Derecskei-Kovacs, A.; North, S. W. *Chem. Phys.* **2000**, *254*, 309.
(57) Li, R.; McGivern, W. S.; North, S. W. *Chem. Phys. Lett.* **2001**, *334*, 47.